

# Negative Resistance and Charge-Density-Wave transport

Lu Mingtao

Supervised by Prof. Dr. Ir. P.H.M. van Loosdrecht

June 6, 2006

## **Abstract**

In reality, there are many ways to get negative resistance, i.e., the charge carriers move in the opposite direction to the applied field. For example: IMPATT diodes, Multiple Quantum Well's, and charge-density-wave (CDW) materials.

The origin of the CDW comes from the periodic overlapping of the Brillouin zone and the Fermi surface. A band gap appears on the energy diagram. The energy cost of lattice deformation is compensated by the lowering of the electronic energy.

Normally, CDW behaves as a semiconductor. Different samples show diverse dc and ac characteristics, like hysteresis, switching or negative differential resistance.

# Contents

## **1. Introduction**

- 1.1 Charge-density-waves and the Peierls transition
- 1.2 Fermi gas and Brillouin zone in 1D, 2D and 3D materials
- 1.3 CDW crystals

## **2. DC characteristics**

- 2.1 Nonlinear dc characteristics
- 2.2 Narrow band noise
- 2.3 Single-particle model
- 2.4 Quasi-particles
- 2.5 Collective excitations
- 2.6 The switching and nonswitching properties of the CDW conductors
- 2.7 Hysteresis

## **3. AC characteristics**

- 3.1 Mode locking and Shapiro steps
- 3.2 Low-frequency and high-frequency ac characteristics

## **4. Negative differential resistance**

- 4.1 Experiment to get N(D)R
- 4.2 Rotating ball model
- 4.3 Explanations for Negative resistance
- 4.4 Negative differential resistance

## **5. Conclusion**

## **6. References**

# 1. Introduction

## 1.1 Charge-density-waves and the Peierls transition

The distribution of particles inside a system is connected with  $kT$ . When the temperature is high, the system is disordered. When temperature is low, the weak interaction inside the system becomes important, the system will become more ordered, combining with a phase transition. Considering electronic phase transitions, a good example in three dimensional materials is superconductivity, in two dimensional materials is Quantum Hall effect. Similarly, a one dimensional electron gas with a finite electron-phonon coupling is unstable and form charge-density-wave (CDW). This phase transition is called Peierls transition. It was first discussed by Fröhlich (1954) and Peierls (1955). The critical temperature at which the transition occurs,  $T_P$ , is determined by the strength of electron-phonon coupling. The appearance of CDW comes from the equilibrium between periodic lattice distortion and periodic modulation of charge density. The latter one is given by

$$n(x,t) = n_0 + \delta n \cos(2k_F x + \phi(x,t))$$

$n_0$  is the charge density without modulation,  $\delta n$  and  $\phi(x,t)$  is the amplitude and phase of the charge modulation.  $k_F$  is the Fermi wavevector which is given by  $k_F = \pi N_e / a$ .  $a$  is the lattice constant,  $N_e$  is the number of electrons per unit cell. The CDW wavelength is  $\lambda_{CDW} = \pi / k_F$ . The period of the modulation is twice the Fermi wave vector ( $Q = 2k_F$ ). An energy gap ( $2\Delta$ ) appears at Fermi surface (See Figure 1). The filled part of the band comes down, and the empty part of the band rises up. The total free energy is lowered.

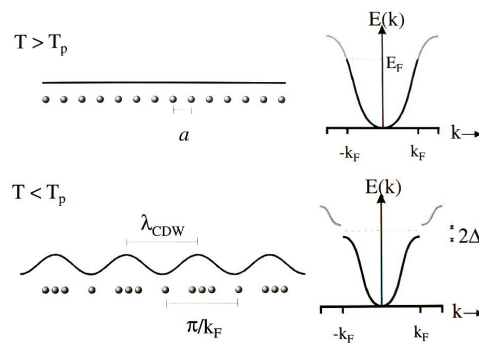


**Figure 1** Simplified representation of an electron spectrum of a one-dimensional metal that undergoes a Peierls transition. For temperatures above the Peierls temperature  $T_P$ , the charge density is uniform. Below  $T_P$ , the lattice is modulated and a Charge-Density-Wave forms. At the Fermi energy, a gap  $2\Delta$  opens. This figure shows the lattice modulation for a commensurate CDW [2].

$\Delta$  is a complex number which represents the order parameter  $\Delta = |\Delta|e^{i\phi}$ .  $|\Delta|$  is the single particle energy gap. This expression is benefit from the order parameter of the super conductor ground state of BCS theory.

Under the condition of electron phonon interaction, the Fröhlich Hamiltonian is written as

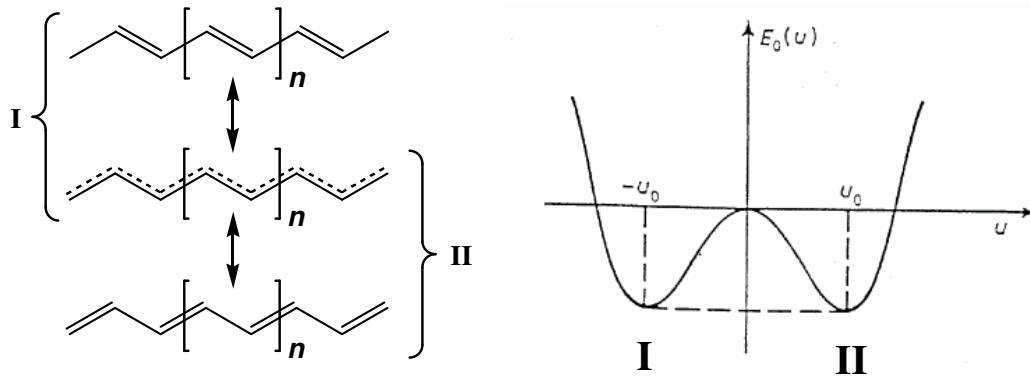
$$H = \sum_k \epsilon_k a_k^\dagger a_k + \sum_q \hbar \omega_q b_q^\dagger b_q + \sum_{k,q} g_q a_{k+q}^\dagger a_k (b_{-q}^\dagger + b_q)$$

Where  $a_k^\dagger a_k$   $b_q^\dagger b_q$  are the creation and annihilation operators of the electrons and phonons,  $g_q$  is the electron-phonon coupling constant:

$$g_q = i \left( \frac{\hbar}{2M \omega_q} \right)^{1/2} |q| V_q$$

$\omega_q$  are the normal mode frequencies.  $M$  is the ionic mass.

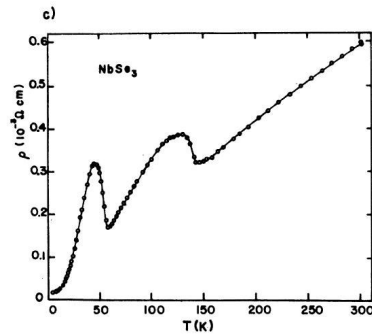
One good example of Peierls transition is polyacetylene. Figure 2 shows three resonant structures of polyacetylene. The state in the middle implies that all the carbon-carbon bonds have the same length. X-ray diffraction shows that there is a bond length alternation of  $0.08\text{\AA}$  inside polyacetylene, i.e., instead of delocalized along the whole chain, the  $\pi$  electrons would like to couple with each other and form  $\pi$  bonds. This gives the two degenerated ground states in the energy diagram (I and II). The middle resonant state is a metastable state setting in between I and II. If there is a perturbation, the system will fall into one of the degenerated ground states.



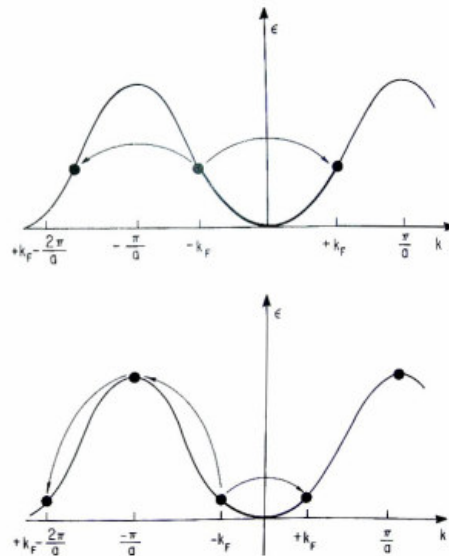
**Figure 2** The two degenerate ground states of polyacetylene [15].

Figure 3 shows a diagram of the resistance of CDW material ( $\text{NbSe}_3$ ) changing with temperature. When temperature is high, the electrons are more easily to be scattered by the lattice vibration. When temperature is decreasing, the resistance also decreases. At 142K and 59K, two Peierls transitions appear. The region where resistance increase with decreasing temperature indicates that the system changes from the metallic state to insulating or semiconducting state (See the

energy diagram in Figure 1). There are three different chain structures in  $\text{NbSe}_3$ , two of them will form CDW at different temperature, that is the reason why two phase transition appear in Figure 3. The third chain has a large chalcogen spacing and does not form CDW at any temperature. The electrons in this chain do not set in the condensed state. This gives a metallic behavior of the  $\text{NbSe}_3$ , since when the temperature goes to zero, the resistance also goes to zero.



**Figure 3** Resistivity of  $\text{NbSe}_3$  vs. temperature. The phase transitions at 145K and 59K have been tentatively identified with the formation of charge-density-waves [7].



**Figure 4** The dispersion relation for a half filled (top part) and one-third filled (bottom part) electron band. The scattering involving the wavevector  $2k_F$  and the scatterings (one in the half filled band and two in the one-third filled band case) which lead to  $\pm k_F - 2\pi/a$  are indicated on the figure by the arrows [6].

If the period of CDW  $\lambda_{\text{CDW}}$  and the lattice constant  $\mathbf{a}$  are commensurate, with a relation of  $\lambda_{\text{CDW}} = (N/M)\mathbf{a}$ , where  $N/M$  is an integer number, the free energy of the system will be reduced by this commensurate effect. For example, if the energy band is half filled, with a momentum of  $Q=2k_F$ , the electrons can be scattered to two directions, either left ( $+k_F - 2\pi/a$ ) or right ( $+k_F$ ) (See

Figure 4). In this case, the system can gain extra energy from the second order terms of the phonon field. Similarly, a system with one-third filled band could gain energy from the third order terms of the phonon field. Note: CDW will not appear if the energy band is filled up.

## 1.2 Fermi gas and Brillouin zone in 1D, 2D and 3D materials

If a positive charge is placed in the free electron gas, the surrounding electrons will be attracted by the positive charge. The total electric field produced by the positive charge will be shielded by the surrounding electrons. This is known as the screening effect. If the induced charge density  $\rho^{ind}$  (the electrons induced by the positive charge) changes linearly with the total potential  $\phi$ ,  $\rho^{ind}(\vec{q}) = \chi(\vec{q})\phi(\vec{q})$ . As long as  $\phi$  varies slowly in  $\mathbf{r}$  space,  $\chi(\mathbf{q})$  can be described by the Lindhard response function:

$$\chi(\vec{q}) = \int \frac{d\vec{k}}{(2\pi)^d} \frac{f_k - f_{k+q}}{\epsilon_k - \epsilon_{k+q}}$$

Where  $f_k = f(\epsilon_k)$  is the Fermi function [11].

The Thomas-Fermi approach is used for dealing with nonlinearly relation between  $\rho^{ind}$  and  $\phi$ , under a condition of very slowly varying external potentials.

For a one-dimensional electron gas, if a perturbation is exerted to the system, the response of the system to this perturbation is assumed to be linear. Near  $2\mathbf{k}_F$  the integral of  $\chi(\mathbf{q})$  in Lindhard function becomes

$$\chi(q) = \frac{-e^2}{\hbar^2 v_F} \ln \left| \frac{q + 2k_F}{q - 2k_F} \right| = -e^2 \mathcal{N}(\epsilon_F) \ln \left| \frac{q + 2k_F}{q - 2k_F} \right|$$

A divergence at  $2\mathbf{k}_F$  appears [See Figure 5]. In this case, at  $q=2k_F$  the system do not linearly response to this perturbation any more, the overall system change from one degenerated ground state to another. Correspondingly, a gap appears on the energy diagram, indicating the Peierls transition.

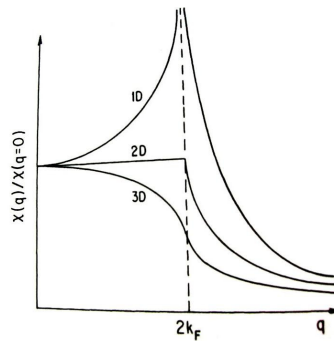


**Figure 5** Wave vector dependent Lindhard response function for 1D, 2D and 3D free electron gas at zero temperature [6]

The coupling of the electron-electron or electron-hole pairs at Fermi surface ( $\pm \mathbf{k}_F$ ) in one dimensional system is described as the following [6]:

$e_+, \sigma; e_-, -\sigma$	pairs with total momentum	$q=0$
	with total spin	$S=0$
$e_+, \sigma; e_-, \sigma$	pairs with	$q=0$
		$S=1$
$e_+, \sigma; h_-, \sigma$	pairs with	$q=2k_F$
		$S=1$
$e_+, \sigma; h_-, -\sigma$	pairs with	$q=2k_F$
		$S=0$

$e_+$ ,  $e_-$  and  $h_+$ ,  $h_-$  indicates the electrons and hole on right or left side. The first two states with  $q=0$  gives the particle-particle or Cooper channel, the last two states with  $q=2k_F$  gives particle-hole channel or Peierls channel.

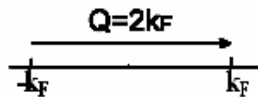


**Figure 6** The Fermi surface of 1D material is two points,  $-k_F$  and  $k_F$ .  $Q$  is the phonon wavevector

For one dimensional material, the Fermi surface is reduced to two points at  $\pm \mathbf{k}_F$  (See Figure 6) [12, 13]. These two points give two degenerated ground states, the scattering of an electron from  $-\mathbf{k}_F$  to  $\mathbf{k}_F$  does not cost energy. But this scattering has to involve momentum. This momentum comes from phonon. If there is a phonon with a momentum of  $Q=2k_F$ , this phonon will be absorbed by the scattering of the electron. This process gives the electron-phonon coupling. For two dimensional and three dimensional materials, similar effect is hard to get, since the Fermi surfaces are not two points anymore (See Figure 7). At  $2\mathbf{k}_F$ , the Lindhard response functions of two dimension and three dimension have finite values (See Figure 5).

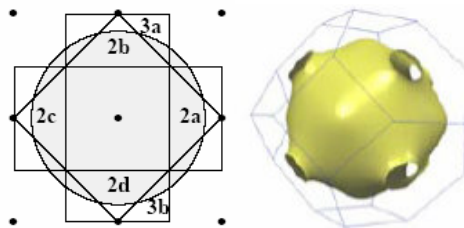


**Figure 7** The Fermi surface and Brillouin zone in 2D and 3D electron gas

There are some exceptions. For example, Figure 8 shows a two dimensional material with a half filled band. A large density of states can contribute to the  $Q=2k_F$  scattering. CDW will also appear, since nesting charges accumulates on the Fermi-surface.

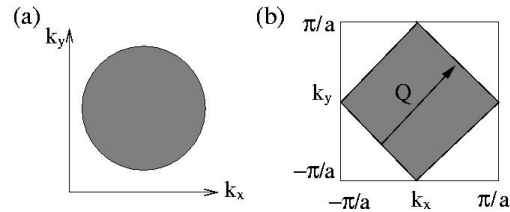


**Figure 8** (a) the Fermi-surface of free electron gas in 2D space (b) the half filled square lattice [30].

### 1.3 CDW crystals

Nowadays, the most famous CDW materials are:

- (1) Mixed valence platinum chain compounds (KCP):  $K_2Pt(CN)_4Br_{0.3}(3H_2O)$
- (2) Transition metalchalcogenides  $MX_3$  ( $M=Ti, Zr, Hf, Nb, Ta; X=S, Se, Te$ ) and  $(MX_4)_nY$  ( $M=Ta, Nb; X=Se, S; Y=I, Br, Cl$ )
- (3) Blue bronze  $A_{0.3}MoO_3$  ( $A=Na, K, Rb, Tl$ ) and purple bronze  $A_{0.9}Mo_6O_{17}$  ( $A=Li, Na, K, Tl$ ) [32]
- (4) Organic charge transfer salt (TTF-TCNQ)
- (5) Tungsten bronzes  $(PO_2)_4(WO_3)_{2m}$  [33]

They all have chain structures with anisotropic conductivity. Along the chain, the conductivity is much larger than perpendicular to the chain. Normally, they are called quasi-one dimensional materials. Some of the structures are showed in Figure 9.

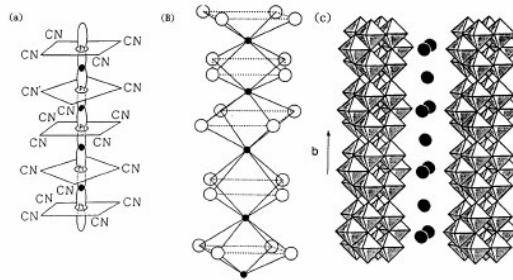


**Figure 9** The chain structure of (a)  $K_2Pt(CN)_4Br_{0.3} \cdot 3.2H_2O$  (b)  $(NbSe_4)_2$  (c)  $K_{0.3}MoO_3$  [6]

Figure 10 shows the crystal structure of  $NbSe_3$ , the Nb atom set a little deviating from the center of the prism. Each Nb atom is adjacent to eight Se atoms, two of them from the neighboring chains. So the coordination number of Nb is eight [6].

The electron configuration of Nb is  $[Kr]4d^45s^1$ , and Se is  $[Ar]3d^{10}4s^24p^4$ . Instead of forming close shell, they combine with each as  $3NbSe_3=2Nb^{5+}Nb^{4+}(Se^{2-})_5(Se_2^{2-})_2$ . The  $d$  orbital of Nb is quarter filled; the whole crystal shows metallic behavior at high temperature.

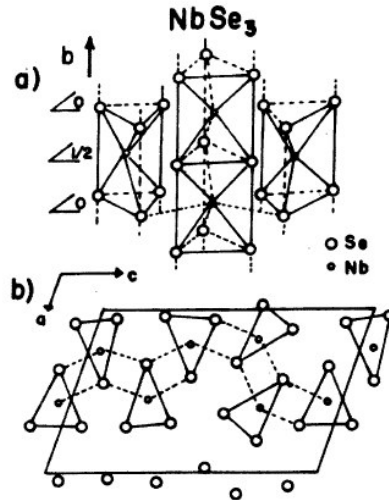


**Figure 10** (a) Crystal structure of NbSe<sub>3</sub> along the b axis. The Nb atoms in the adjacent chains are displaced by half lattice spacing along b with respect to each other. (b) Crystal structure of NbSe<sub>3</sub> in the a-c plane. The unit cell, comprised of six prisms and represented by the parallelogram, has the dimensions  $a=10.006\text{\AA}$ ,  $b=3.478\text{\AA}$ ,  $c=15.626\text{\AA}$ ,  $\beta=109.30^\circ$ . The Nb-Nb distance along b is  $3.478\text{\AA}$  (compared to  $2.68\text{\AA}$  in the metal). In the other direction it varies from  $4.45$  to  $4.25\text{\AA}$ . The dashed lines connect Nb and Se atoms in the same plane [7].

## 2. DC characteristics

The nonlinear response to the dc field, hysteresis and narrow band noise (NBN) are the typical dc characters of CDW. The dc response of the CDW material largely depends on such properties as the size of the sample, the impurity density, or the grain boundaries. The reason for this is that these defects or confinements break the coherence of the CDW collective modes. Some impurities have large electron affinities, the screening effect will reduce the electron density in the sample; the strength of the pinning center will also affect the CDW transport. These different effects give diverse I-V line shapes.

### 2.1 Nonlinear dc characteristics

DC characteristics describe the response of CDW to the applied dc electric field. Normal metals have linear response to the applied field. In CDW state, the conductivity of the material is field dependent, due to the pinning effect. Typical dc current-voltage characteristic is showed in Figure 11. At low field, the conductivity obeys Ohm's law.  $\sigma$  (the conductivity measured at 130K) is 500 times smaller than  $\sigma_{RT}$  (the conductivity measured at room temperature, used for normalization). Because at low temperature, most of the electrons are setting in the condensate state and form CDW, the density of free electrons is relatively low. Note the material showed in Figure 11 is o-TaS<sub>3</sub>, which has a different transport property with NbSe<sub>3</sub>, showed in Figure 3 (just opposite to o-TaS<sub>3</sub>, at low temperature the conductivity of NbSe<sub>3</sub> is high). At high field, both the quasi-particle

and CDW will contribute to the total current. There is a threshold field  $E_T$  setting in between. The smoothly changing of the conduction at  $E_T$  means the crystal is nonswitching, which will be discussed later. Above  $E_T$ , the onset of nonlinear conduction can be observed.

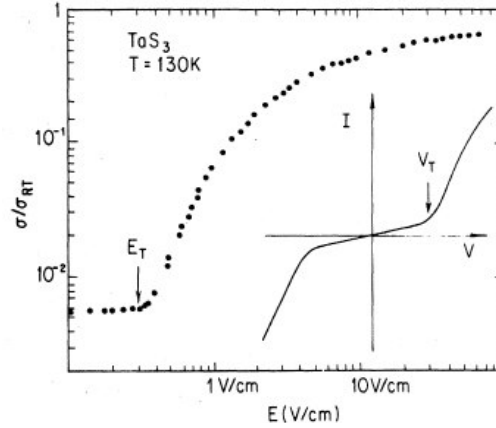


**Figure 11** Electric-field-dependent cordial conductivity  $\sigma_c(E)$  in o-TaS<sub>3</sub> in the CDW state. The data are normalized to the room-temperature conductivity. The insert shows typical dc I-V characteristics on the same material [14].

## 2.2 Narrow band noise

The Narrow band noise (NBN), which is also called current oscillation, suggests the coherence of the current throughout the sample. The correlation range  $\langle j(t, \mathbf{0}), j(t, \mathbf{r}) \rangle$  is associated with the dimensions of the sample.

If the applied current or voltage is fixed, the narrow band noise will appear in the output signal while the applied field is larger than the threshold field  $E > E_T$  (See Figure 12). The Fourier transform is the way to change signal from time dependence to frequency dependence.

The board band noise indicates the nonlinear of the CDW conduction caused by the macroscopic grain boundaries, and the periodic appearing of the narrow band noise comes from the single particle rolling down the washboard potential (will be discussed later in single particle model). The higher is the applied voltage, the higher is the frequency of NBN. The NBN frequency is given by

$$f_{NBN} = \frac{j_{CDW}}{n_c e \lambda_{CDW}}$$

$j_{CDW}$  is CDW current density,  $n_c$  is the concentration of the condensed carriers,  $\lambda$  is the CDW wavelength. (Note: the origins of the narrow band noise are different for  $\text{K}_{0.3}\text{MoO}_3$  and for  $\text{NbSe}_3$ , as will be discussed later)

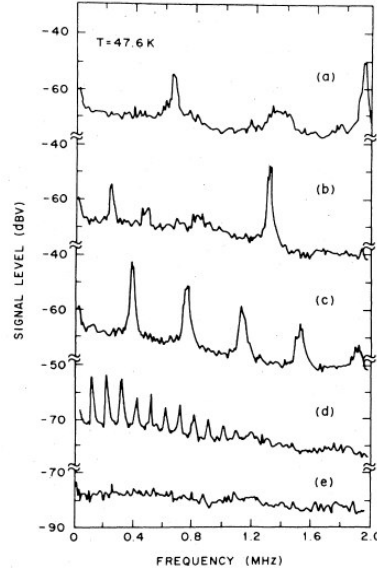


**Figure 12** Fourier transform of the time-dependent current in NbSe<sub>3</sub> or various applied currents. Narrow-band “noise” results if the current exceeds the threshold value for the nonlinear conduction. Current exceeds the threshold value for nonlinear conduction. Currents and dc voltage are (a)  $I=270 \mu\text{A}$ ,  $V=5.81\text{mV}$ ; (b)  $I=219 \mu\text{A}$ ,  $V=5.05\text{mV}$ ; (c)  $I=154 \mu\text{A}$ ,  $V=4.07\text{mV}$ ; (d)  $I=123 \mu\text{A}$ ,  $V=3.40\text{mV}$ ; (e)  $I=V=0$ . The sample cross-sectional area  $A \approx 136 \mu\text{m}^2$  [14].

The coherence of the current oscillations is given by the quality factor  $Q = \Delta_f / f_0$ .  $\Delta_f$  is the width of the fundamental.  $f_0$  is the frequency of the single particle velocity (See Figure 12). There is a relation between the width of the narrow band noise and the amplitude of the broad band noise: the smaller the broad band noise amplitude, the larger the  $Q$ . The depasing of the CDW domains gives the time dependence of the oscillation amplitude. The relation between current and frequency is given by [6]

$$\frac{j_{CDW}}{f_0} = ce \frac{n_{CDW}(T)}{n_{CDW}(T=0)}$$

$J_{CDW}$  is the current per CDW chain carried by the condensate.  $c$  is constant.

### 2.3 Single-particle model

A number of models have been developed to illustrate CDW switching. Joos and Murray proposed a domain coupling model [21]; Janossy and Kriza suggested a CDW self-blocking mechanism [22]; Hall et al. have given a single-degree-of-freedom model with inertia [19], Wonnerberger has proposed a single-degree-of-freedom model with current noise [23]. All of them failed to give a correct explanation, because they neglected the amplitude of fluctuation. However, among them, the single particle model is the most popular canonical model. The idea

comes from the classical motion of a single particle [6]. In this case, the whole CDW is considered as one single particle (See Figure 13). It is pinned on a periodic potential by impurities.

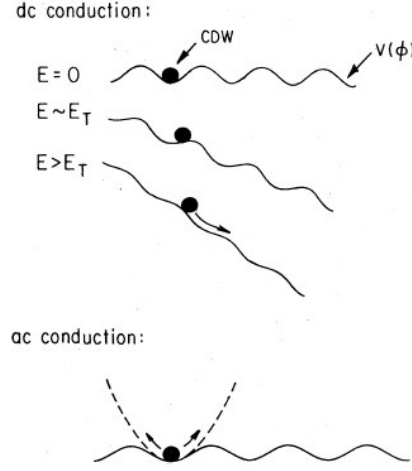


**Figure 13** Classical particle model of charge density wave transport [14]

The origin of this periodic potential may be different for different materials. In  $K_{0.3}MoO_3$  it comes from the uniformly distributed impurities inside the sample, in  $NbSe_3$  it comes from the underlying lattice. When the applied field is small ( $E < E_T$ ), the CDW is still pinned there. When the applied field is large ( $E > E_T$ ), the CDW is depinned and start to move. The velocity of the single particle is not a constant, but modulated by a frequency of  $\omega_0$ , where  $\omega_0$  is the pinning frequency representing the strength of the impurity potential. This pinning frequency gives the narrow band noise showed in Figure 12. The periodic potential is given by

$$U(x) = \frac{m^* \omega_0^2}{4k_F^2} (1 - \cos(2k_F x))$$

The motion of the single particle is given by

$$\frac{d^2 x}{dt^2} + \frac{\gamma_0}{m^*} \frac{dx}{dt} - \frac{\omega_0^2}{2k_F} \sin(2k_F x) = \frac{e}{m^*} E_x$$

Where  $\gamma_0$  represents the damping coefficient which appears when CDW interacts with quasi-particles.  $x$  is the CDW center-of-mass coordinate,  $t$  is a time variable,  $m^*$  is the Fröhlich mass of the CDW electrons, and  $E_x$  is the applied electric field. Typically  $m^*$  is 100 to 2000 times larger than  $m_e$ , the inertial term is negligible because the phase relaxation rate (order of  $10^{-11}$  s) is much faster than either  $\omega_0$  or the frequency of the applied electric field. From this equation, the conductivity of the sample can be calculated. The imaginary part of the conductivity describes the CDW that is scattered during transport.

Under small dc electric field, the electrons in the condensate of CDW do not contribute to the conduction process. The interactions with impurities shift the oscillator strength associated with the collective modes to finite frequencies (the collective mode will be introduced later). The applied small dc field induces a translational motion of the condensate, called sliding density wave transport.

The Hamiltonian describes the interaction between impurities and the collective mode is  $H=V\cos(2k_Fx+\Phi)$ . where  $V(x)=\omega_0\sin 2k_Fx/2k_F$ , gives the impurity potential which pins the density wave to the underlying lattice. The various potentials  $V(r)$  break the translational invariance of the collective modes.

The total Hamiltonian is given by  $H=H_{el}+H_E+H_\Delta+V_{imp}(\Phi)$ .

$H_{el}$  represents the gradient energy,  $H_\Delta$  is the energy related with small amplitude fluctuation,  $H_E$  is the potential energy density,  $V_{imp}$  is the impurity potential [6].

## 2.4 Quasi-particles

In the single particle model, the concept of the quasi-particle has been used. It comes from Landau's treatment of weakly-interacting electrons in a conductor. This treatment is the famous formulation known as weakly-interacting electrons. The quasi-particle can be treated as a moving particle interacting with the environment. The other surrounding particles may be pushed away or dragged along by its motion. The moving electrons interact with each other by Coulombic force. Most of the interactions can be included in the effective mass of a single particle. Then it can be treated as a free electron, which is called quasi-particle. In this way, the many-body problem can be simplified to a one-body problem. Sometimes, quasi-particles may not obey the energy conservation and the Pauli Exclusion Principle.

The quasi-particle represents a low lying excited state of the system, i.e., quasi-particle is the renormalized single particle excitation. If we treat the quasi-particle as a point source, the field generated by the point source can be expressed as Green's function. The imaginary part of the self-energy gives the life time of the quasi-particle. If there is no interaction between quasi-particles, the life time of the quasi-particle will be infinitely large.

## 2.5 Collective excitations

In a many body system, besides quasi-particle, there is another kind of fictitious particle, i.e., collective excitations. Particles like plasmons, phonons or magnons are all collective excitations. In charge-density-wave, there are two collective modes: amplitude mode and phase mode. Figure 14 clearly shows that only phase mode could contribute to the CDW transport. In single particle model, the shape of the ball (single particle) is assumed to be unchanged, so only phase mode is

involved, the amplitude mode does not contribute to the total transport. These collective excitations can be measured by optic method. The phase mode is Raman inactive but IR active, since there is no electron gas deformation in it. The amplitude mode is Raman active.

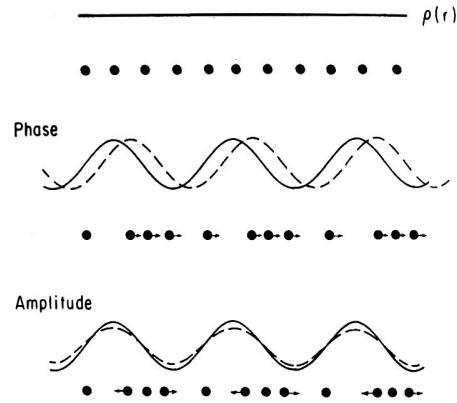


**Figure 14** Amplitude (A) and phase ( $\phi$ ) excitations of the charge density wave state in the  $q=0$  limit. Charges of both the charge density and ionic displacements are indicated. The upper part of the figure shows the charge density and the atomic positions in the metallic state [6].

$$\Delta(x,t) = [|\Delta| + \delta(x,t)]e^{i\phi(x,t)}$$

These collective modes can be involved in the order parameter:

$|\Delta|$  is the single particle energy gap as described before.  $\delta(\mathbf{x},\mathbf{t})$  gives the amplitude fluctuation.  $\phi(\mathbf{x},\mathbf{t})$  gives the phase fluctuation. This time-dependent order parameter of the CDW excitation states can be explained by Ginzburg-Landau theory.

If there is no commensurate effect, the translation motion of CDW will not change the condensation energy of the system. In small specimen with size comparable to phase-phase correlation length  $L_\phi$ , the internal deformation is not important; the single particle model still works well. If only weak pinning impurities exist in the sample, the amplitude of CDW can be treated as constant. On the other hand, if the strong pinning center dominates the sample, the amplitude collapse and phase slip occur at the pinning site.

The threshold field  $E_T$  increases with increasing impurity concentrations. For strong pinning,  $E_T \sim n_i$ ; for weak pinning,  $E_T \sim n_i^2$ . The total current is given by  $I_{tot} = I_n + I_{CDW}$ .  $I_n$  is the Ohmic contribution that comes from the uncondensed electrons,  $I_{CDW}$  is the nonlinear response that comes from the condensed electrons. For  $E > E_T$ , the CDW executes a translational motion, the amplitude of CDW remains unchanged.

## 2.6 Switching and nonswitching properties of CDW conductors

According to the dc characteristics research of A. Zettl, two kinds of CDW conductor are nominated: switching and nonswitching [1]. Normally, CDW is pinned by the impurities in the sample. It could also be depinned by an applied electric field  $\mathbf{E}$  larger than the threshold field  $\mathbf{E}_T$ .

In nonswitching materials, CDW current depins smoothly with increasing  $E$ . In the case of switching, an abrupt step appears at the critical field  $E_c$ , with  $E_c = E_T$ .

Switching can be gotten by reducing the cross-sectional area of the nonswitching crystal, thereby shortening the width of the crystal to the same order with CDW phase-coherence length. The CDW current can not flow around localized regions any more, and will result in an onset of CDW motion. In switching crystal, the critical threshold field  $E_c$  is independent of temperature. Comparing with nonswitching, many dramatic phenomenon appears in switching: hysteresis [25], negative differential resistance [26], bistability and large  $1/f$  noise [26], an inductive ac response [27], and period-doubling routes to chaos [29]. The origin of switching is still unclear. One explanation is that it comes from the amplitude collapse and phase slip of the CDW at the strong pinning centers in the sample. If the temperature is a finite value but not zero, the pinning effect of small center will be reduced by thermal activation. Since switching is related with nonuniform distribution of strong pinning centers, it is independent of temperature (still under the condition of low temperature).

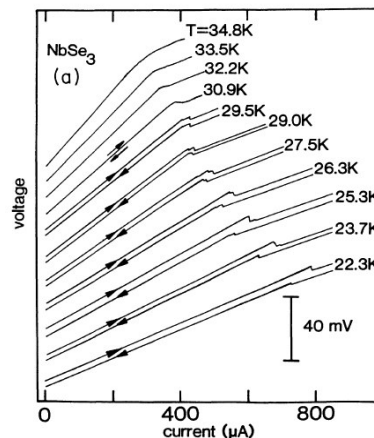


**Figure 15** Current-driven dc I-V curves for a switching crystal of NbSe<sub>3</sub>. Arrows indicate the direction of bias sweep. For temperature below 30K, the traces for forward- and reverse- bias sweeps have been vertically offset for clarity [1].

## 2.7 Hysteresis

Figure 15 shows the hysteresis of the I-V curve. One way to explain this hysteresis effect is that the CDW domains will change when the applied electric field changes. The nonuniform pinning of the impurities breaks the coherence of the CDW and separates the crystal into different domains.

As the applied electric field increases, part of the weak pinning effects are overcome (See Figure 16), the average domain size increases. On the other hand, if the applied electric field decreases from a high value, the domain size will decrease and the CDW has to overcome these pinning

centers again, but in the opposite direction. This gives the hysteresis. Because the domain size is much smaller than the size of the sample, the step of the domain size changing can not be detected by the I-V measurement. Since we can not quantitatively measure the strength and density of the pinning impurities, this explanation is not fully verified.

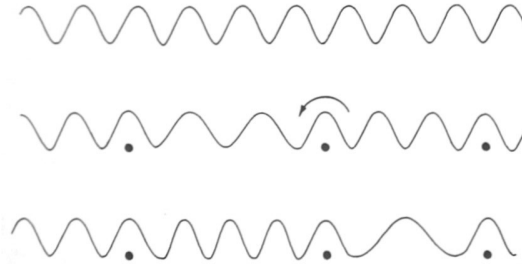


**Figure 16** The dynamics of the internal deformations of density waves. The top part of the figure is the undistorted density wave; the middle part shows the mode distorted due to the interaction with impurities (full circles); and the bottom part displays the rearrangement of the internal distortion by the displacing the density wave by period over the impurity as indicated by the arrow. The process leads to an internal polarization [6].

### 3. AC characteristics

In some experiments, dc and ac fields are applied to the sample simultaneously. The response of ac field can be used to value the effective mass  $m^*$ , the pinning frequency  $\omega_0$  and damping constant  $1/\tau$ . The nonlinear responses of dc effects are showed in chapter 2. The dc conductivity is  $\sigma_{dc} = \langle j(t) \rangle / E_{dc}$ .  $E_{dc}$  is the applied electric field,  $\langle j(t) \rangle$  is the time average current. The ac conductivity is  $\sigma_{ac} = \text{Re}\{\sigma(\omega)\} + i\text{Im}\{\sigma(\omega)\}$ .

$\text{Re}\{\sigma(\omega)\}$  and  $\text{Im}\{\sigma(\omega)\}$  are the real and imaginary part of the ac conductivity. The ac field is given by  $E_{ac} = E_0 \sin \omega t$ . The total voltage is  $V = V_{dc} + V_{ac} \cos(\omega t)$ . The ac response may be linear or nonlinear, depending on the frequency.

ac current method can also be used to measure the narrow band noise frequency. When both frequency of ac current and NBN are matching with each other, mode locking occurs. Correspondingly, Shapiro steps appear on the I-V characteristics and peaks appear on the differential resistance measurements.

#### 3.1 Mode locking and Shapiro steps

The Shapiro phenomena were first used to demonstrate the ac Josephson Effect of Josephson junctions. Same method can also be used in a CDW system. The combined ac and dc current are applied to the sample. While the ac current frequency coincides with narrow band noise frequency, the CDW velocity is fixed by the applied ac current, voltage steps appear in the current-voltage characteristic and peaks appear in the differential resistance. If the CDW is fully

mode-locked by the ac current, the voltage steps will become horizontal and the peaks will have same height (See Figure 17). The height of the  $n^{\text{th}}$  step is given by [6]

$$\Delta I(\omega) \approx 2I_J(\omega=0) \left| \frac{J_n I_1(\omega)}{\omega I_1(\omega=0)} \right|$$

$J_n$  is the Bessel function of order  $n$ .

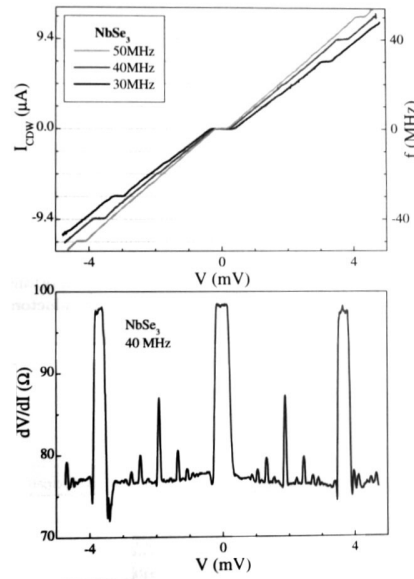


**Figure 17** Shapiro step measurement on NbSe<sub>3</sub> at T=120K. The current-voltage characteristics show clear voltage steps where the CDW mode-locks to the external frequency. These voltage steps correspond to the peaks in the differential resistance. The step height  $\Delta I_{\text{CDW}}$  is proportional to the applied frequency  $f$  [2].

Subharmonic Shapiro steps appear when  $p f_{\text{ext}} = q f_0$ .  $q$  is an integer other than one.  $f_{\text{ext}}$  is the applied ac current frequency.  $f_0$  is the NBN frequency. The subharmonic Shapiro steps are labeled by  $p/q$ , since they are  $p/q$  times of the fundamental in  $I_{\text{CDW}}-\omega_{\text{ext}}$  diagram (See Figure 18)

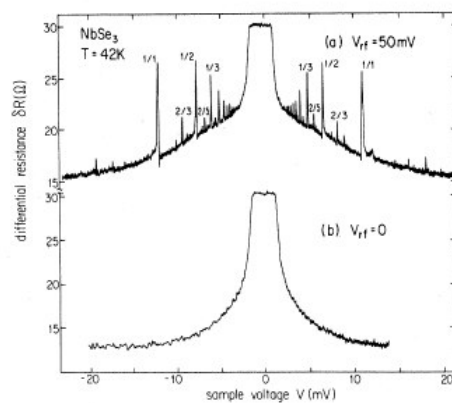


**Figure 18** Differential resistance of NbSe<sub>3</sub> with and without an applied rf voltage  $V_{\text{rf}}$ . The numbers indicate the various subharmonic steps (Brown et al., 1984)

### 3.2 Low-frequency and high-frequency ac characteristics

With no frequency dispersion coming from uncondensed electrons in NbSe<sub>3</sub>, the conductivity of the lower CDW state (below 59K) is given by

$$\sigma_{CDW} = I_{ac} / V_{ac} - \sigma_0$$

$\sigma_0$  is the low-field dc conductivity of the crystal (due to uncondensed electrons).

CDW shows different ac characteristics at different temperature. At 47K, the in-phase part of the conductivity (Re  $\sigma_{CDW}$ ) is zero at low frequency and increases with increasing frequency. The out-of-phase part of the conductivity (Im  $\sigma_{CDW}$ ) is a finite value at low frequency and keeps increasing with increasing frequency and begin to decrease again for frequencies past 200MHz. At 24K, both Re  $\sigma_{CDW}$  and Im  $\sigma_{CDW}$  increase monotonically with increasing frequency (See Figure 19).

In Zettl's paper, rigid-phase model is used to analysis ac characteristics [8]. In this model the CDW amplitude is fixed and the phase is uniform. The equation of motion is given by

$$\frac{d^2\phi}{dt^2} + \frac{1}{\tau} \frac{d\phi}{dt} + \omega_0^2 F(\phi) = \frac{e}{m^*} EQ$$

$\omega_0$  is the frequency representing the strength of the CDW pinning.  $F(\phi)$  is the pinning force that can be approximated to its first Fourier component  $F(\phi) = \sin(\phi)$ . Then the motion equation can be rewritten as  $\beta\ddot{\phi} + \dot{\phi} + F(\phi) = e_{dc} + e_{ac} \cos(\Omega t)$

$\beta$  is the inertia parameter given by  $\beta = (\omega_0 \tau)^2$ ,  $\Omega = \omega / (\omega_0 \tau)^2$ ,  $e_{ac} = E_{ac} / E_T$ ,  $e_{dc} = E_{dc} / E_T$ , where  $E_T = m^* \omega_0^2 / eQ$ .

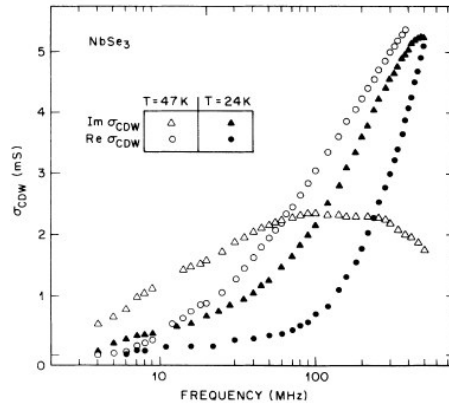


**Figure 19** The zero-bias, complex conductivity of the crystal. Circle and triangles indicate the in-phase and out-of-phase components of conductivity, respectively. Open and solid symbols indicate data taken at 47K and 24K, respectively [8].

The two part of the conductivity is given by

$$\text{Re } \sigma(\Omega) = \frac{ne^2\tau}{m^*} \frac{\Omega^2}{(1 - \beta\Omega^2)^2 + \Omega^2}$$

$$\text{Im } \sigma(\Omega) = \frac{ne^2\tau}{m^*} \frac{\Omega(1 - \beta\Omega^2)}{(1 - \beta\Omega^2)^2 + \Omega^2}$$

When  $\beta$  is small, CDW dynamics is overdamped. When  $\beta$  is large, CDW dynamics is underdamped. The  $\sigma$ - $\Omega$  diagram shows Lorentzian line shape (See Figure 20).

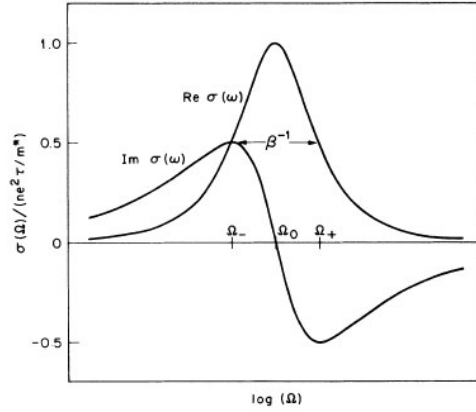


**Figure 20** The zero-bias pinned ac conductivity of the classical, rigid-phase of CDW dynamics [8].

Three characteristic frequencies are showed the in Figure 20:

$$\Omega_0 = \beta^{-1/2}$$

$$\Omega_{\pm} = (\sqrt{1 + 4\beta} \pm 1) / 2\beta$$

$\Omega_0$  is the normalized pinning frequency.  $\Omega_{\pm}$  are the frequency corresponding to  $\text{Im}\sigma = \pm \text{Re}\sigma$ .

For frequencies between zero and  $\Omega_-$ , the CDW conductivity is capacitive; between  $\Omega_-$  and  $\Omega_+$ , the CDW conductivity is dissipative; between  $\Omega_+$  and  $\infty$ , the CDW conductivity is inductive. The measurement showed in Figure 19 is in the capacitive regime. The fitting parameter of  $0 \leq \beta \leq 0.2$  shows that the CDW motion is pinned and overdamped at 24K.

## 4. Negative resistance and negative differential resistance

### 4.1 Experiment to get N(D)R

When measurements are carried out at a length scale less than  $1\mu\text{m}$ —the typical domain width scale, unordinary phenomena can be expected. Actually, such experiments have been done by van der Zant in 2001. Surprisingly, some measurements show negative resistance, i.e., the charge carriers go in the opposite direction to the applied electric field.

The way to get NR is to deposit the CDW crystal on insulating substrate bearing metal probes. The probes are etched by e-beam to 100nm in width and 50nm in height. The smallest separation of

two probes is 300nm (See Figure 21). On top of the CDW layer, two electrodes are attached to it by glue.

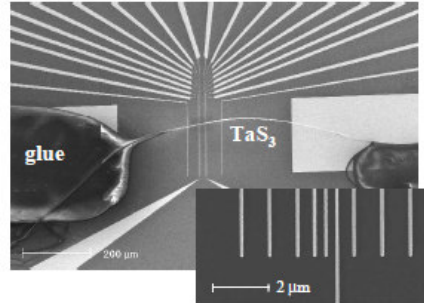


**Figure 21** A thin  $\text{TaS}_3$  crystal on top of an array of voltage probes to study CDW dynamics on submicron length scales. The spacing between the big (current) pads on either side of the picture is 0.5mm. The inset shows an enlargement of the main figure with 9 voltage probes that are 100nm wide; the smallest distance between adjacent probes is 300nm. Each sample has two of these probe-sets that separated 12 $\mu\text{m}$  from each other [31].

The I-V characteristics of the four-terminal measurement are showed in Figure 22. The results are very different from segments to segments. Some segments give typical nonlinear response, others show negative differential resistance, or even negative absolute resistance in I-V curve. The dash line is the average of different segments. It matches with the I-V curve measured on larger length scales, i.e., the total tendency of the charge carriers go in the same direction with the applied field, while at some small length scales, negative resistance can be observed.

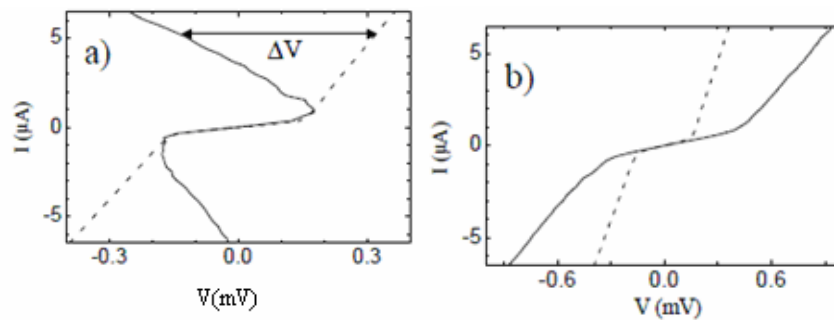


**Figure 22** Two current-voltage characteristics of a  $\text{TaS}_3$  crystal with a cross section of  $0.5\mu\text{m}^2$ . The curves are taken at 120K on adjacent  $1\mu\text{m}$ -long segments. Dashed lines correspond to a measurement on a  $31.6\mu\text{m}$  long segment for which the voltage has been scaled by a factor of  $1/31.6$ . They represent the expected, averaged nonlinear CDW behavior. In a) the absolute value of the resistance becomes negative for high positive bias. The deviation  $\Delta V$  from the expected behavior is linear in  $I_{\text{CDW}}$ . The curve in b) shows less CDW current at a given field, i.e., it is less nonlinear. When adding up the two curves one approximately recovers the expected, average CDW behavior [31].

## 4.2 Rotating ball model

The phenomenon of NR obeys the Energy Conservation theory and the Principle of Entropy increase. Just like a ball can not move from the bottom to the top of the slant by itself. But in some certain condition, we can see the ball moving upward.

Suppose we have a ball which has a center of gravity deviating from the geometry center. We put the ball on the slant as showed in Figure 23. If the gravity force is large enough to overcome the moving downward momentum of the ball, then the ball will temporarily move upward.

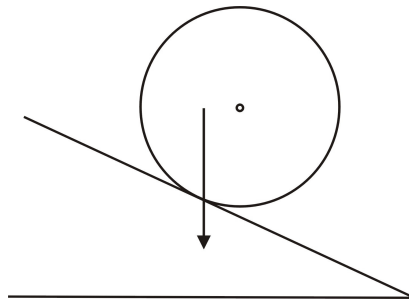


**Figure 23** A solid ball with the center of gravity deviate from the center of the geometry.

Following this idea, maybe a similar effect as negative resistance can also be found in mechanics. Same ball with the one showed in Figure 23, but some tricks have been done on it. The region **A** which is showed by the bold line in Figure 24 has a larger friction constant than the other part of the ball and it will temporarily move upward under the condition showed in Figure 24.

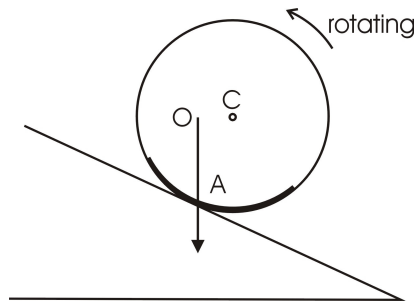


**Figure 24** The temporarily moving upward of the ball

As the gravity force is setting in the same line of the geometry center of the ball, the torque becomes zero; the velocity of the ball also decreases to zero at a certain point. At the exact moment, because the friction constant of the ball touching the slant is small, the ball begins to slide downwards with slight rotation, as shown in Figure 25.

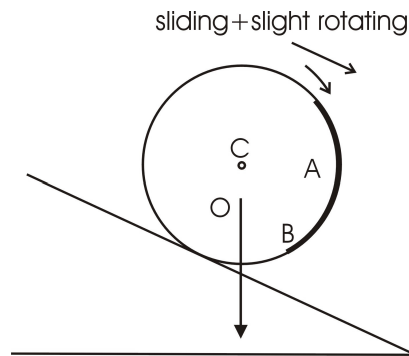


**Figure 25** Sliding and slightly rotating of the ball

As the B point (the starting point of zone A showed in Figure 25) becomes the touching point, the ball moves with a motion of full rotation. Because of the inertia of the ball, it will move downward for a short range (See Figure 26), and then start to move upward and repeat the process from Figure 24 again.

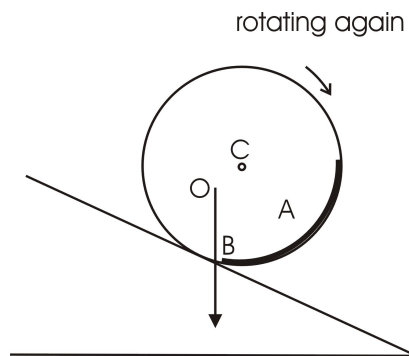


**Figure 26** The downward rotating of the ball

For the whole process, the total tendency of the ball is moving downward. But at certain small length scale, the upward motion of the ball can be observed. If the ball starts at the same point each time, the moving upward of the ball can always be observed at the same position of the slant, which is the similar with the position of the CDW where the NR is observed. In the CDW, this trick is played by the quasi-particle. All the charge carriers are considered together as a ball here. In o-TaS<sub>3</sub>, most of the electrons set in the condensate state and form CDW. So the main part of the ball is consisted by CDW (represented by the smooth part of the ball). The unsmooth part of the ball (region A) represents the quasi-particle. The range of the region is the life time of the quasi-particle. The gravity potential represents the applied field. The total current is given by  $j=Nev$ . The negative velocity of the ball gives the negative resistance. In the NR region, the ball spends more time on moving upward than moving downward. Similarly, the time average output voltage measured between neighboring probes gives negative resistance.

The designed experiment to prove this idea shows as following: Use the same CDW sample and make any two neighboring probes have same distance throughout the sample. The negative resistance should be observed periodically in a short length scale (depends on the size of the current domain).

### 4.3 Explanations for negative resistance

There are many explanations for the negative resistance, here two are given. The first one is that inside the two dimensional sample, vortex will form around strong pinning center (Figure 27b). This vortex will force the charge carriers go in the opposite direction to the applied field.

Another explanation is that the CDW and quasi-particle are driven by different forces (Figure 27a). The CDW is related to electric potential  $\Phi$ , and the quasi-particle is related to electrochemical potential  $U$ . If there is a strong pinning center inside the sample, Phase slip and amplitude collapse may occur at this center. The high charge density near the strong pinning center will give a high electrochemical potential, which drives charge carriers to the opposite direction.

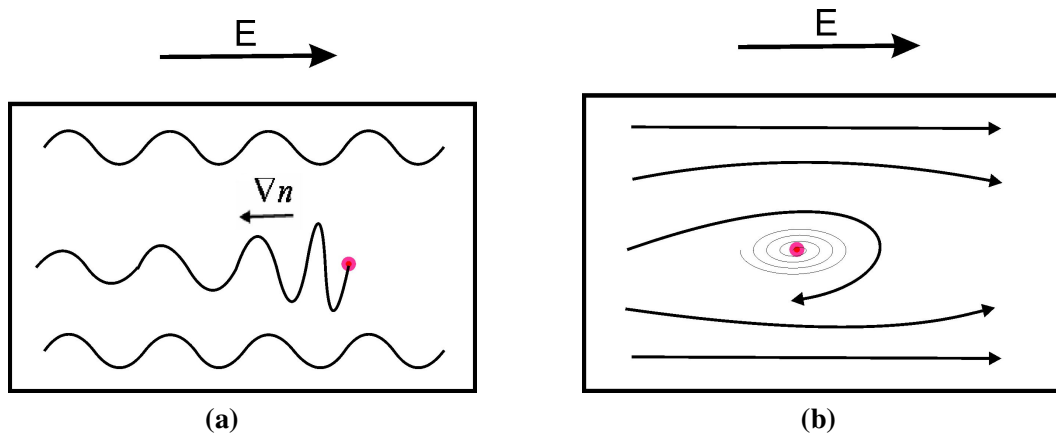


**Figure 27** (a) The CDW and quasi-particle are driven by different force. (b) The vortex forming around strong pinning center forces charge carriers to go backward.

Quasi-particle is the most effective way here to describe this process. As the temperature decreases,  $N(D)R$  becomes more pronounced. Because if the temperature increases, the quasi-particles are more easily to be scattered, their life time will decrease correspondingly.

The potential and current distributions along the sample are showed in Figure 28. The total current is given by  $I=I_q+I_{CDW}$ . The quasi-particle current is given by  $I_q=\sigma_q dU/dx$ .  $\sigma_q$  is the linear conduction per unit length. The CDW current is given by  $I_{CDW} =K \dot{\phi}$ , where  $\phi$  is the CDW phase and  $K$  is constant. Normally, the electrochemical potential is smaller than the electric potential. In the NR region, the electrochemical potential wins. The Fermi surface in NR region has to adjust

itself to keep charge neutral. The shift of the chemical potential  $\mu$  is given by  $\mu=(U-\Phi)$ .  $\mu$  is proportional to  $d\phi/dx$ .

In NR region, CDW current changes to  $I_{CDW} = (1+\alpha) K \dot{\phi}$ ,  $\alpha$  is given by  $\alpha=\Delta V/(R_0 I_{CDW})$ .

$\alpha$  is related to the quasi-particle life time. Since the total current is constant, we get  $K \dot{\phi}+I_q=(1+\alpha) K \dot{\phi}+V/R_0$ ,  $R_0$  is the resistance of the sample. In NR region, the voltage is given by

$V=R_0(I_q-\alpha I_{CDW})$ . If  $I_{CDW}> I_q/\alpha$ ,  $V$  becomes negative. The NR effect can not be observed while the distance of the segments is larger than a critical value  $l_{max}$ .  $l_{max}$  is related to the CDW phase-slip voltage.

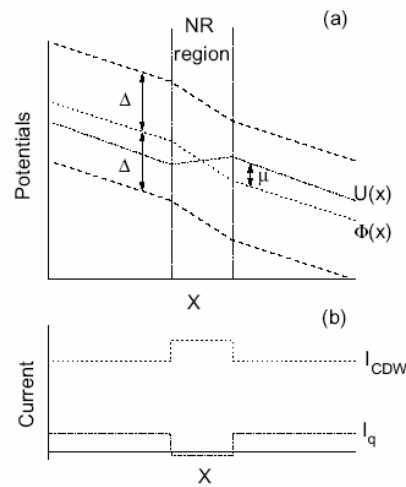


**Figure 28** (a) Band bending and (b) current distributions around the NR region.  $\Phi$  coincides with the middle of the Peierls gap under the chosen calibration of the electrostatic potential. Edges of the Peierls gap are represented by the dashed lines [31].

During the whole process, the CDW act as a spring which is periodically elongated or pressed. This process expressed by the negatively or positively velocity of the CDW phase  $\phi$ . The spring constant is given by  $\dot{\phi}$ . Since the periodic time of elongation and press are different, the time average of the measurements of two probes may give a negative resistance. The force exerting on the spring comes from the phase accumulation of the CDW (the nonuniform of the charge density  $\nabla n$ ), the phonon (the periodically changing of the lattice by the net current of CDW) and the applied electric field.

#### 4.4 Negative differential resistance

Negative differential resistance (NDR) can be observed in the I-V measurement of an NbSe<sub>3</sub> single crystal at T=40K (See Figure 29). NDR appears somewhat above threshold current  $I_T$ . A remarkable feature of this NDR is that it is temporal instable.

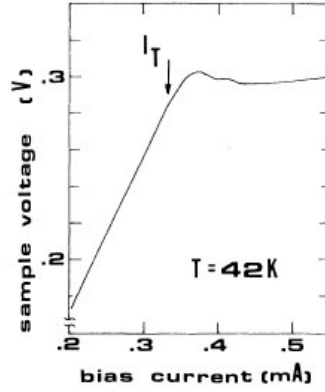


**Figure 29** I-V characteristics of NbSe<sub>3</sub>. The arrow indicates the threshold current. A negative differential resistance is clearly observed near threshold [19].

In Zettl's opinion, the CDW crystal can be treated as a two-fluid model [20]. The current is consisted with electrons with two different conductances: the field-independent conductance  $\sigma_N$  and field-dependent conductance  $\sigma_{CDW}$ . With increasing the applied electric field, the  $d\sigma_{CDW}/dV$  is always larger than zero. NDR can never be gotten in a voltage-driven CDW. The current-voltage relation is given by

$$I = [\sigma_N + \sigma_{CDW}(V)]V$$

The differential conductance is given by

$$\frac{dI}{dV} = [\sigma_N + \sigma_{CDW}(V)] + \frac{d\sigma_{CDW}(V)}{dV}$$

The differential conductance is always positive.

In current-driven CDW, the current-voltage relation is given by

$$V = \frac{I}{\sigma_N + \sigma_{CDW}(I)}$$

The differential resistance is given by

$$\frac{dV}{dI} = \frac{1}{\sigma_N + \sigma_{CDW}(I)} - \frac{I\sigma'_{CDW}(I)}{[\sigma_N + \sigma_{CDW}(I)]^2}$$

NDR can be gotten when

$$\sigma'_{CDW}(I) > \frac{\sigma_N + \sigma_{CDW}(I)}{I}$$

Near threshold, the  $\sigma_{CDW}$  is less than  $\sigma_N$ , this condition can be satisfied. NDR occurs at a temperature setting in between switching and nonswitching. In NDR region, the applied current depins only part of the CDW which is depinned continuously but rapidly increasing with increasing applied current.

## 5 Conclusions

Phase transitions are the battle between order and disorder. Heat is the source of disorder. When temperature is low and order wins, a new phase will appear. In the boson-fermion system, there are many ways to calculate the ground state of the system.

Since many comparable effects of superconductors can also be found in CDW, the low-dimension system has its special priority to make certain complicated conditions simple. The diverse ac and dc characteristics under different conditions give a large research space in this area. However, the density and strength of the impurities, which plays an essential role in CDW transport, can not be measured directly. Further experimental improvements need to be made to prove the various assumptions. In spite of this, there is already a big progress. With the technique of Focused-Ion beam etching, the separation of two probes can be reduced to less than  $1\mu\text{m}$ . This is a critical size for CDW transport. At this range, the negative differential resistance and negative absolute resistance can be observed clearly. Although these phenomena are seemingly unreasonable, they occur in the real world. Up to now, the smallest width of the wire is  $65\text{nm}$  in the semiconductor industry. One can imagine if the distance of two probes is in the same order with the CDW wavelength ( $\sim 1\text{nm}$ ), more fantastic phenomenon may appear.

The rotating ball model is a parody of the single particle mode. The collective mode is not included in the model. The complication of many-body interaction always makes things insoluble. The quasi-particle is an effective way to reduce many-body problem to one-body problem. But this way brings a new problem: the single particle has to interact with itself. This is similar with the radiation reaction in quantum field theory. Anyway, the Fermi Liquid theory, along with BCS theory, is one of the most successful theories in physics.

A rough calculation of the NR has been presented by van der Zant, but exactly how the electrochemical potential is driving the quasi-particle to move in the opposite direction to the applied electric field is still unclear. With applying electric field on the sample and the impurities pinning the CDW, phase slip and amplitude collapse may occur. The Hamiltonian is always very complicated and insoluble. All kinds of approaches have been made to describe CDW motion. The canonical single particle is showed in chapter 2.

In recent twenty years, Peierls transition have been synthesized and observed in many low-dimensional materials. A large space is available for further research in this region.

## 6 References:

- [1] R.P. Hall, M.F. Hundley, and A. Zettl, Phys. Rev. B 38, 13002 (1988)
- [2] Erwin Slot, Microscopic Charge Density Wave Transport (2005)
- [3] Richard Mattuck, A guide to Feynman diagrams in the many-body problem.
- [4] L.C. Kimerling, Heterogeneous Equilibria Preparation of Solid State Materials
- [5] R. M. Fleming, D. E. Moncton and D. B. McWhan, Phys. Rev. B 18, 5560 (1978);
- [6] George Grüner, Density Waves in Solids (1994)
- [7] N. P. Ong and Monceau, Phys. Rev. B 16, 3443 (1977)
- [8] R. P. Hall and A. Zettl, Phys. Rev. B 38, 13019 (1988)
- [9] C.J. Pethick and H. Smith, Bose-Einstein Condensation in Dilute Gases (Cambridge, New York 2002).
- [10] KOTOMIN E A, CHRISTENSEN N E, EGLITIS R I. A comparative study of the atomic and electronic structure of F centers in ferroelectric  $\text{KnbO}_3\text{:Ab}$  initio and semi-empirical calculations[J]. Computational Materials Science, 1998, 10:339-345.
- [11] Neil W. Ashcroft, N. David Mermin, Solid State Physics
- [12] Solyom, J., 1979, Adv. Phys. 28, 201
- [13] Emery, V., 1979, in Highly Conducting One-Dimensional Solids, edited by J. Devreese et al. (Plenum Press; New York, London)
- [14] G. Grüner, Reviews of Modern Physics, Vol. 60, No.4, October 1988
- [15] Bart de Boer, Opto-Electronic Properties of Polymers (Part 2)
- [16] H. Fukuyama, J. Phys. Soc. Jpn. 41, 513 (1976)
- [17] H. Fukuyama and P. A. Lee, Phys. Rev. B 17, 535 (1978)
- [18] P. A. Lee and T. M. Rice, Phys. Rev. B 19, 3970 (1979)
- [19] R.P. Hall and A. Zettl, Phys. Rev. B 30, 2279 (1984)
- [20] M. S. Sherwin and A. Zettl, Phys. Rev. B 38, 13028 (1988)
- [21] B. Joos and D. Murray, Phys. Rev. B 29, 1094 (1984)
- [22] A. Janossy, G. Mihaly and L. Mihaly, in Ref. 12, p. 412.
- [24] W. Wonneberger and H. J. Breymayer, Z. Phys. B 56, 241 (1984)
- [25] A. Zettl and G. Grüner, Phys. Rev. B 26, 2298 (1982)
- [26] R. P. Hall, M, S, Sherwin, and A. Zettl, Phys. Rev. Lett. 52, 2293 (1984)
- [27] R. P. Hall and A. Zettl, Solid State Commun. 55, 307 (1985)
- [28] M. Sato, H. Fujishita, and S. Hoshino, Solid State Commun. 49, 313 (1984)
- [29] R. P. Hall, M, S, Sherwin, and A. Zettl, Phys. Rev. B 29, 7076 (1984)
- [30] D. W. Wang, et. al., cond-mat/0410494

- [31] H. S. J. van der Zant, E. Slot, S. V. Zaitsev-Zotov and S. N. Artemenko, *Phys. Rev. Lett.* **87**, 126401 (2001)
- [32] A. W. McConnell, B. P. Clayman, C. C. Homes, M. Inoue and H. Negishi, *Phys. Rev. Lett.* **58**, 13565 (1998)
- [33] J. Dumas, C. Hess, C. Schlenker, G. Bonfait, E. Gomez Marin, D. Groult and J. Marcus, *Eur. Phys. J. B* **14**, 73-82 (2000)